

Published in final edited form as:

Epilepsia. 2014 August ; 55(8): 1274–1283. doi:10.1111/epi.12657.

Antiepileptic Activity of Preferential Inhibitors of Persistent Sodium Current

Lyndsey L. Anderson^{1,*}, Christopher H. Thompson^{2,*}, Nicole A. Hawkins², Ravi D. Nath², Adam A. Petersohn², Sridharan Rajamani³, William S. Bush⁴, Wayne N. Frankel⁵, Carlos G. Vanoye^{2,*}, Jennifer A. Kearney², and Alfred L. George Jr^{1,2,*}

¹Department of Pharmacology, Vanderbilt University, Nashville, TN, USA

²Department of Medicine, Vanderbilt University, Nashville, TN, USA

³Gilead Sciences Inc., Fremont, CA, USA

⁴Department of Biomedical Informatics, Vanderbilt University, Nashville, TN, USA

⁵The Jackson Laboratory, Bar Harbor, ME, USA

Abstract

Objective—Evidence from basic neurophysiology and molecular genetics has implicated persistent sodium current conducted by voltage-gated sodium (Na_V) channels as a contributor to the pathogenesis of epilepsy. Many antiepileptic drugs target Na_V channels and modulate neuronal excitability mainly by a use-dependent block of transient sodium current, although suppression of persistent current may also contribute to the efficacy of these drugs. We hypothesized that a drug or compound capable of preferential inhibition of persistent sodium current would have antiepileptic activity.

Methods—We examined the antiepileptic activity of two selective persistent sodium current blockers ranolazine, an FDA-approved drug for treatment of angina pectoris, and GS967, a novel compound with more potent effects on persistent current, in the epileptic *Scn2a*^{Q54} mouse model. We also examined the effect of GS967 in the maximal electroshock model and evaluated effects of the compound on neuronal excitability, propensity for hilar neuron loss, development of mossy fiber sprouting and survival of *Scn2a*^{Q54} mice.

Results—We found that ranolazine was capable of reducing seizure frequency by ~50% in *Scn2a*^{Q54} mice. The more potent persistent current blocker GS967 reduced seizure frequency by greater than 90% in *Scn2a*^{Q54} mice and protected against induced seizures in the maximal electroshock model. GS967 greatly attenuated abnormal spontaneous action potential firing in

Correspondence: Alfred L. George, Jr., M.D., Division of Genetic Medicine, 529 Light Hall, Vanderbilt University, 2215 Garland Avenue, Nashville, TN 37232-0275, Tel: 615-936-2660, Fax: 615-936-2661, al.george@vanderbilt.edu.

*current address Department of Pharmacology, Northwestern University Feinberg School of Medicine, Searle 8-510, 320 East Superior Avenue, Chicago, IL 60611, al.george@northwestern.edu

DISCLOSURES

Dr. Rajamani is a fully time employee of Gilead Sciences, Inc., which manufactures and hold patent rights to both ranolazine and GS967. Dr. George received research funding for this study from Gilead Sciences, Inc. No other author has any disclosures.

We confirm that we have read the Journal's position on issues involved in ethical publication and affirm that this report is consistent with those guidelines.

pyramidal neurons acutely isolated from *Scn2a*^{Q54} mice. In addition to seizure suppression *in vivo*, GS967 treatment greatly improved the survival of *Scn2a*^{Q54} mice, prevented hilar neuron loss, and suppressed the development of hippocampal mossy fiber sprouting.

Significance—Our findings indicate that the selective persistent sodium current blocker GS967 has potent antiepileptic activity and this compound could inform development of new agents.

Keywords

Epilepsy; sodium channel; mossy fiber sprouting; neurophysiology

INTRODUCTION

Epilepsy is a common neurological disorder affecting approximately 1% of the world's population.^{1–3} Antiepileptic drugs (AEDs) are the mainstay of treatment for most patients and several mechanistically distinct classes of agents are available. Unfortunately, 30% of persons affected by epilepsy fail to achieve adequate seizure control with currently available pharmaceuticals suggesting the need for new AEDs.³

Many widely used and successful AEDs target voltage-gated sodium (Na_v) channels, typically by mechanisms resulting in use-dependent block of transient sodium current. Persistent sodium current, a small non-inactivating component of overall current carried by Na_v channels, may be another potential target for AED action. Neurons in several brain regions exhibit persistent sodium current and this activity may help amplify subthreshold synaptic potentials and facilitate repetitive firing.⁴ Further, increased persistent sodium current is an observed feature of several heterologously expressed mutant human Na_v channels associated with familial epilepsy syndromes such as genetic epilepsy with febrile seizures plus (GEFS+).⁵ Ranolazine is an FDA-approved drug for the treatment of angina pectoris arising from coronary insufficiency and acts by preferentially inhibiting persistent sodium current in heart. We previously reported that ranolazine can suppress persistent current generated by several human Na_v1.1 mutations associated with genetic epilepsies or familial hemiplegic migraine.⁶ Ranolazine has also been shown to reduce action potential firing and epileptiform activity in cultured neurons.⁷ Whether preferential suppression of persistent sodium current would be antiepileptic *in vivo* is unknown.

The genetically engineered mouse line, *Scn2a*^{Q54}, expresses a transgene encoding an inactivation-impaired neuronal Na_v1.2 channel. Mice expressing the *Scn2a*^{Q54} transgene exhibit a severe epilepsy phenotype that is characterized by short-duration partial seizures beginning in early life that then progress to secondarily generalized seizures, status epilepticus and premature death.^{8,9} Epilepsy in *Scn2a*^{Q54} mice is correlated with increased persistent sodium current in hippocampal neurons. These animals also exhibit histopathologic changes in the hippocampus, including hilar neuron loss and mossy fiber sprouting that also occur in chronic human epilepsy. This animal model provides an excellent opportunity to test the efficacy of drugs targeting persistent sodium current. We hypothesized that preferential inhibition of persistent sodium current would eliminate sodium channel dysfunction and exert an antiepileptic effect in *Scn2a*^{Q54} mice.

In this study, we investigated the antiepileptic effect of preferential persistent sodium current inhibition using ranolazine and the recently described novel compound, GS967.^{10,11} We observed that both ranolazine and GS967 reduced seizure frequency in *Scn2a*^{Q54} mice, and GS967 inhibited spontaneous action potential firing in neurons isolated from *Scn2a*^{Q54} mice. GS967 was also effective at protecting against seizures in the maximal electroshock (MES) model. Additionally, we found that long-term treatment with GS967 greatly improved survival, prevented hilar neuron loss and suppressed the development of mossy fiber sprouting in *Scn2a*^{Q54} mice.

EXPERIMENTAL PROCEDURES

Animals

All animal care and experimental procedures were approved by the Vanderbilt University Institutional Animal Care and Use Committee, and the principles outlined in the ARRIVE guidelines and the Basel declaration were considered when planning experiments. Mice were group-housed in a specific pathogen free mouse facility under standard laboratory conditions (12-h light/dark cycle). Mice had access to food and water *ad libitum*, except during experiments. *Scn2a*^{Q54} transgenic mice were generated as previously described and are maintained as a congenic line on the C57BL/6J background (B6.Q54).⁹ For experiments, F1 generation mice were produced by crossing B6.Q54 hemizygous transgenic males with SJL/J females. Genotyping of the *Scn2a*^{Q54} transgene was performed as previously described.⁸ Experimental animals used in this study were males age 30–35 days unless otherwise noted.

Acute isolation of hippocampal neurons

Electrophysiology experiments were performed on acutely dissociated hippocampal pyramidal neurons isolated from *Scn2a*^{Q54} mice. We used acutely dissociated neurons because they afford for a greater degree of voltage control necessary to accurately measure persistent sodium current and allow for direct application of drugs. Hippocampal neurons were isolated as previously described.¹² Pyramidal neurons were identified based on morphological criteria, with a pyramidal shaped cell body and a long apical process as previously described.¹²

Electrophysiology

Mutagenesis of recombinant rat Na_v1.2 (rNa_v1.2) was performed as described previously.^{13–15} Three mutations (G879Q, A880Q, L881Q) were introduced into full length rNa_v1.2 to recapitulate the *Scn2a*^{Q54} transgene. Heterologous expression of rNa_v1.2 in tsA201 cells and whole cell voltage clamp recording were performed as previously described.¹⁶ Whole-cell voltage clamp and current clamp recordings of neuronal cell bodies were performed as described previously.¹² All voltage clamp recordings utilized a holding potential of –90 mV. Persistent sodium current was measured during the final 10 ms of a 200 ms depolarization to –10 mV from the holding potential in the absence and presence of 1 μM GS967 or 10 μM phenytoin, followed by application of 0.5 μM tetrodotoxin (TTX) and offline digital subtraction as described previously.⁶ Use-dependent rundown was measured at stimulation frequencies of 10, 30, and 100 Hz in the absence and presence of

either 1 μM GS967 or 10 μM phenytoin, followed by application of 0.5 μM TTX and offline digital subtraction of TTX-resistant current. For current clamp recordings, membrane potential was clamped to -80 mV and cells were allowed to fire spontaneously. Spontaneous action potential firing frequency of neurons isolated from both male and female mice was measured in the absence and presence of GS967 (100, 300 and 1000 nM) or phenytoin (1000 nM). Statistical comparisons were made using either Student t-test or one-way ANOVA followed by Tukey's post-test and $p < 0.05$ was considered statistically significant.

Evaluation of anticonvulsant activity in *Scn2a*^{Q54} mice

Anticonvulsant activity was evaluated by comparing the number of behavioral seizures captured by video recording during a 30-min pre-treatment period with the number occurring during a 30-min post-drug period in male *Scn2a*^{Q54} mice. Pre- and post-treatment periods were collected between 8:00 – 10:30 a.m. for all experimental animals. Behavioral seizures (tonic deviation of the head and body accompanied by forelimb clonus) were previously correlated with electroencephalographic seizures using video-EEG monitoring,⁹ and work in our laboratory has demonstrated a strong correlation between behavioral and electroencephalographic seizures ($\kappa = 0.988$) in untreated mice. Mice were implanted with prefabricated headmounts (Pinnacle Technology, Inc., Lawrence, KS, USA) for video-EEG monitoring as previously described.¹² Video-EEG data was collected from ranolazine treated mice. Mice were placed in individual recording cages for 60-min prior to a randomly assigned drug treatment (30-min habituation followed by 30-min pre-treatment period). Mice received 40 mg/kg ranolazine (maximum tolerated dose) or PBS as a single i.p. injection and were immediately returned to the recording cage for the 30-min post-treatment period. Phenytoin experimental animals received a single i.p. injection of either 30 mg/kg phenytoin, which produced a plasma concentration within the human therapeutic range, or vehicle and were returned to the home cage for a delay of 75-min. Mice were then placed into the recording cage for 30-min habituation followed by the 30-min post-treatment period. The delay between drug injection and post-treatment period for each drug was based upon the time to peak plasma ranolazine concentration and the previously determined time to peak phenytoin effect.¹⁷ GS967 could not be administered satisfactorily by the i.p. route because the vehicle alone caused excessive sedation in mice, and the stress of intravenous or oral gavage administration would have exacerbated seizures in *Scn2a*^{Q54} mice. Therefore, GS967 was administered orally through supplementation in chow. Baseline seizure frequency was quantified for 30 minutes in the GS967 experimental group (pre-treatment period), then mice were returned to the home cage and received either control or GS967 containing chow (either 2 mg drug per kg chow or 8 mg drug per kg chow; dosage estimated as 0.375 mg/kg/d and 1.5 mg/kg/d, respectively, based on the consumption of 3.5–4 g chow per day). Mice had access to either control or GS967 chow *ad libitum*. Plasma and whole brain was isolated from all experimental animals immediately following the post-treatment period. Digital video images captured during the 30-min video-monitored periods (pre- and post-drug treatment) were analyzed offline by two independent observers blinded to treatment, and percent change in seizure frequency was calculated. Statistical comparisons were made using repeated measures ANOVA and $p < 0.05$ was considered statistically significant. Statistical analysis was conducted using STATA 12.0 (StataCorp LP, College Station, TX).

Maximal electroshock-induced seizures

MES experiments were performed at The Jackson Laboratory (Bar Harbor, ME, USA) using nine week old C57BL/6J male mice. Mice were administered either GS967 or phenytoin solutions by oral gavage in a volume of 10 ml/kg body weight two hours prior to MES testing. All tests were conducted at the empirically determined time to peak GS967 effect and previously determined time to peak phenytoin effect.¹⁷ Electrical stimuli was administered using transcorneal electrodes as previously described.¹⁸ Maximal seizures begin with tonic extension of the forelimbs and terminate with tonic hindlimb extension. Maximal seizures were scored with full tonic hindlimb extension (hindlimbs at 180 degree angle to the torso) as the endpoint. Probit analysis was used to determine ED₅₀ with half maximal effective concentration (ED₅₀) values for GS967 and phenytoin.

Survival Analysis

At weaning (postnatal day 21), *Scn2a*^{Q54} mice were randomly assigned to either GS967 or control treatment groups. Animals in the GS967 treatment group were provided chow containing GS967. Survival was monitored until 12 weeks of age. Statistical comparisons were made using the Cox proportional hazards model and $p < 0.05$ was considered statistically significant.

Histology

Cresyl Violet and Timm staining were used to detect hilar neuron loss and mossy fiber sprouting, respectively, in the dentate gyrus of female mice (age 60–65 days). At weaning (postnatal day 21), *Scn2a*^{Q54} mice were randomly assigned to either GS967 or control treatment groups, and animals in the GS967 experimental group were provided chow containing GS967 (8 mg/kg) until the morning of sacrifice. An untreated group of WT littermates were also included. Staining with Cresyl Violet was performed as previously described.⁹ Timm staining was performed as previously described.¹⁹ Mossy fiber sprouting was compared among groups using one-way ANOVA followed by Tukey's post-hoc test and $p < 0.05$ was considered statistically significant.

RESULTS

Ranolazine reduces seizure frequency in *Scn2a*^{Q54} mice

Previous work in heterologous cells demonstrated that ranolazine preferentially suppressed persistent sodium current induced by several human Na_v1.1 mutants.⁶ Here we tested the ability of ranolazine to reduce seizure frequency *in vivo* using *Scn2a*^{Q54} mice that have seizures as a consequence of an abnormal neuronal persistent sodium current conducted by a mutant Na_v1.2 transgene. Seizure frequency was quantified for 30 minutes before and after intraperitoneal administration of 40 mg/kg ranolazine or vehicle. Ranolazine reduced seizure frequency significantly compared to vehicle treated animals (Fig. 1). Additionally, a subset of animals (n=9) were monitored with simultaneous video-EEG recording. Following acute ranolazine treatment, we found a 98% correlation between electroencephalographic and behavioral seizures (55 behavioral vs 56 electroencephalographic) and this was not different from untreated animals. The proportional reduction in seizure frequency was modest (48%)

possibly due to short plasma half-life (~15 minutes) and low brain penetration of ranolazine in mice (Table 1). Despite the pharmacokinetic limitations of ranolazine, these results provided a proof-of-principle that preferential suppression of persistent sodium current can exert an antiepileptic effect.

GS967 inhibits persistent current and spontaneous action potential firing

The novel compound, GS967, has recently been shown to selectively inhibit persistent sodium current mediated by the cardiac voltage gated sodium channel with much greater potency than ranolazine. Further, GS967 exhibited no cross reactivity with cardiac ion channels and several other molecular targets (in total more than 600 studied targets) at 1 μM , albeit effects on ion channels expressed in the brain were not been specifically examined.¹⁰ To investigate the effects of GS967 on brain Na_V channels, we performed whole-cell voltage clamp recordings on tsA201 cells expressing a mutant $\text{Na}_V1.2$ cDNA derived from the *Scn2a*^{Q54} transgene (rat $\text{Na}_V1.2$ -GAL879-881QQQ). External application of GS967 suppressed persistent sodium current with an estimated half maximal inhibitory concentration (IC_{50}) of $0.44 \pm 0.16 \mu\text{M}$, while peak (transient) current was inhibited with an estimated IC_{50} of $18.7 \pm 47.2 \mu\text{M}$ (solubility limits of GS967 precluded testing concentration higher than 10 μM) indicating a 42-fold greater preference for persistent current block over peak current block ($p < 0.05$; Fig. 2A, C). For comparison, phenytoin, a commonly prescribed AED, also inhibited persistent current (IC_{50} of $15.9 \pm 24.7 \mu\text{M}$ vs IC_{50} of $143.7 \pm 70.1 \mu\text{M}$, $p < 0.05$; Fig 2B, C), but with lower potency and less preference (9-fold) over peak compared to GS967. Additionally, application of 1 μM GS967 induces small hyperpolarized shifts in the voltage dependence of activation and steady-state inactivation, and slows the fast component of recovery from fast inactivation (Supplementary Fig. 1, Supplementary Table 1).

A common feature of several AEDs is use-dependent inhibition of transient sodium current. Therefore, we examined use-dependent inhibition of $\text{Na}_V1.2$ -GAL879-881QQQ mediated sodium current by either 1 μM GS967 or 10 μM phenytoin at different frequencies (10 – 100 Hz). We observed minimal steady-state use-dependent inhibition by GS967 across the range of stimulation frequencies (Fig. 2D), consistent with the activity of this drug observed on the cardiac voltage gated sodium channel.¹⁰ However, as expected, phenytoin exhibited strong use-dependent block of transient sodium current (Fig. 2D), with a greater degree of inhibition at high stimulation frequencies ($44.2 \pm 3.7\%$) compared to low frequency stimulation ($22.6 \pm 2.8\%$, $p < 0.05$). These data suggest that GS967 acts mainly through a tonic block mechanism to preferentially inhibit persistent sodium current.

We next investigated whether GS967 could exert preferential suppression of persistent sodium current in neurons isolated from *Scn2a*^{Q54} mice and whether this effect would inhibit neuronal action potential firing. Persistent current measurements from hippocampal pyramidal neurons isolated from *Scn2a*^{Q54} mice demonstrated that 1 μM GS967 significantly reduced persistent current from $1.2 \pm 0.4\%$ of peak current amplitude ($n = 8$) measured under control conditions to $0.1 \pm 0.1\%$ ($n = 5$, $p < 0.05$; Fig. 3A,B). Whole-cell current clamp recording was then performed on hippocampal pyramidal neurons in the presence and absence of GS967. Neurons isolated from *Scn2a*^{Q54} mice exhibited high

frequency spontaneous action potential firing, unlike non-transgenic wild-type littermates that exhibit rare spontaneous firing (Fig. 3C). Application of 1 μ M GS967 reduced firing frequency by $98.8 \pm 0.1\%$ ($n = 7$) and this effect was reversible upon washout of the compound. Suppression of neuronal firing by GS967 was concentration-dependent, with an estimated IC_{50} of ~ 250 nM (Fig. 3D). By comparison, 1 μ M phenytoin inhibited spontaneous action potential firing by only $36.7 \pm 10.1\%$ (open square in Fig 3D).

Based on these *in vitro* observations coupled with the ability of GS967 to effectively cross the blood-brain barrier (Table 1), and a slower rate of elimination than ranolazine, we hypothesized that GS967 would exert antiepileptic activity *in vivo*. Accordingly, we examined the effect of GS967 *in vivo* using two mouse models of epilepsy.

Seizure frequency in *Scn2a*^{Q54} mice is reduced by GS967

First, we tested the ability of short-course (1–2 days) oral GS967 to reduce seizure frequency in *Scn2a*^{Q54} mice. Mice maintained on 0.375 mg/kg/d GS967 exhibited a 50% reduction in seizure frequency whereas mice treated with higher dose (1.5 mg/kg/d) GS967 exhibited more than 90% seizure reduction following two days of treatment (Fig. 4A,B). The efficacy of this compound to suppress seizures in *Scn2a*^{Q54} mice is similar to phenytoin (30 mg/kg), but the anticonvulsant effect of GS967 requires a much lower plasma concentration (Table 1). Vehicle controls for both GS967 and phenytoin treated animals exhibited no reduction in seizure frequency. It was observed that mice treated with phenytoin exhibited sedation characterized by lack of ambulation. Although there was a trend toward sedation, it was not significantly different from vehicle treated mice. By contrast, no sedation was observed in GS967 and respective control treated animals.

GS967 suppresses MES-induced seizures

To further investigate the antiepileptic activity of GS967, we tested the ability of the compound to prevent MES-induced generalized tonic hindlimb seizures in wild-type C57BL/6J mice. Varying dosages of GS967 that yielded 0 to 100% protection were orally administered two hours prior to testing. Protection of MES-induced tonic hindlimb extension by GS967 was dose-dependent (Supplementary Fig. 2), with a calculated ED_{50} value of 0.1 mg/kg. Vehicle treatment exhibited no protection against MES-induced seizures. For comparison, we experimentally determined an ED_{50} value of ~ 5 mg/kg for phenytoin protection against MES-induced tonic hindlimb extension consistent with previously published data.¹⁷ These observations indicate that GS967 has antiepileptic activity in two mechanistically divergent models of epilepsy.

GS967 improves survival of *Scn2a*^{Q54} mice

Scn2a^{Q54} mice have a significantly reduced lifespan with approximately 20% surviving to 12 weeks of age (Fig. 4C). Poor survival of *Scn2a*^{Q54} mice has been attributed to chronic, unrelenting seizures with widespread neuronal injury. We tested whether preferential suppression of persistent current by GS967 would increase the lifespan of *Scn2a*^{Q54} mice. Mice were continuously treated with GS967 beginning at postnatal day 21 and survival was monitored until 12 weeks of age. GS967 treatment dramatically improved the survival of

Scn2a^{Q54} mice with 90% of mice alive at 12 weeks compared to 20% survival of control (untreated) animals ($p < 0.005$; Fig. 4C).

GS967 treatment prevents hilar neuron loss

Widespread neuronal loss in the dentate hilus is a commonly observed histopathological change in epilepsy patients and animal models of epilepsy, including the *Scn2a*^{Q54} mouse model.^{9,20,21} We investigated whether chronic GS967 treatment would prevent neuron loss in *Scn2a*^{Q54} mice. Cresyl Violet staining revealed extensive neuronal cell loss in the dentate hilus in 60 day-old *Scn2a*^{Q54} mice compared to age-matched wild-type (WT) littermates (Fig. 5A–C) as reported previously.⁹ By contrast, qualitatively, there was no overt hilar neuron loss in GS967 treated *Scn2a*^{Q54} mice, indicating that GS967 treatment provides a neuronal preservation effect possibly by attenuating excitotoxicity caused by persistent sodium current.

Mossy fiber sprouting is suppressed by GS967 treatment

Seizure-induced sprouting of the mossy fiber pathway in the dentate gyrus is a frequently observed morphological change associated with epilepsy²¹ and has also been observed in *Scn2a*^{Q54} mice.⁹ We tested whether chronic GS967 treatment of *Scn2a*^{Q54} mice would attenuate mossy fiber sprouting. Using Timm staining, we observed evidence of robust mossy fiber sprouting within the inner molecular layer of the dentate gyrus in 60 day-old *Scn2a*^{Q54} mice compared to age-matched WT littermates (Fig. 5D,E). By contrast, *Scn2a*^{Q54} mice chronically treated with GS967 exhibited a low density of Timm staining (Fig. 5F). Mossy fiber sprouting was quantified in the inner molecular layer of the dentate gyrus using densitometry normalized to background staining. There was a significant ($p < 0.05$) reduction in the extent of mossy fiber sprouting in GS967 treated *Scn2a*^{Q54} mice (1.32 ± 0.12) compared to untreated *Scn2a*^{Q54} (1.81 ± 0.16) and WT (1.36 ± 0.07) animals. These findings indicate that chronic seizure suppression by GS967 prevents mossy fiber sprouting in *Scn2a*^{Q54} mice.

DISCUSSION

In this study, we determined the antiepileptic effect of ranolazine and GS967, two persistent sodium current blockers. AEDs targeting voltage-gated sodium channels have existed for many years, and most exert their clinical effects through use-dependent block of transient sodium current in a manner similar to that of local anesthetics. Use-dependent block of the transient sodium current can dampen neuronal excitability especially during rapid firing such as the hypersynchronous bursts associated with seizures. While some AEDs may also suppress persistent sodium current to some extent, no currently approved AED has a strong preference blocking this activity.²²

Persistent sodium current and epilepsy

Under normal physiological conditions, opening of voltage-gated sodium channels is short-lived and lasts only a few milliseconds before the process of fast inactivation returns current levels to near baseline values. However, a small amount of sodium current may persist after the main transient current is extinguished. This persistent sodium current can influence

neuronal firing by amplifying subthreshold synaptic inputs or evoking a sustained membrane depolarization.⁴ The ability of persistent sodium current to promote neuronal excitability has led to speculation that this current may contribute to epilepsy possibly by allowing pathological firing frequencies or by enabling the spread of epileptic neuronal activity.

Several lines of evidence support the hypothesis that persistent sodium current can be epileptogenic. Mutations in human Nav1.1, Nav1.3 and Nav1.6 sodium channels have been associated with a spectrum of genetic epilepsies. *In vitro* experiments probing the functional consequences of several human mutations have revealed increased persistent sodium current as a major, and sometimes solitary, defect.^{13,14,23–26} Further, low level expression of a mutant Nav1.2 transgene exhibiting increased persistent current in the *Scn2a*^{Q54} mouse model demonstrates the pathogenic nature of this current.⁹ Additionally, Chen and colleagues demonstrated high-threshold bursting in hippocampal CA1 neurons is driven by persistent sodium current in the pilocarpine-induced status epilepticus rat model of temporal lobe epilepsy.²⁷ The authors speculate that increased persistent sodium current contributes to establishing chronic epilepsy in this rodent model. More recently, evidence from *Drosophila* demonstrate important contributions of persistent neuronal sodium current to seizure phenotypes arising from spontaneous and engineered mutants.^{28,29} While increased persistent current does not account for all genetic epilepsies arising from mutant sodium channels, this mechanism appears to be an important contributor in many situations.

Antiepileptic activity of GS967

GS967 has previously been shown to preferentially inhibit persistent sodium current mediated by the cardiac voltage gated sodium channel and is an effective suppressor of ventricular arrhythmias.^{10,11} Unlike ranolazine, GS967 is capable of effectively penetrating the blood brain barrier and has slow elimination from the body, suggesting that this compound may have more efficacious antiepileptic activity. Our data show that GS967 was capable of preferentially suppressing persistent sodium current mediated by a neuronal voltage gated sodium channel with greater potency than the commonly prescribed AED phenytoin, and inhibited spontaneous action potentials in pyramidal neurons isolated from *Scn2a*^{Q54} mice. Importantly, GS967 suppressed seizures from both *Scn2a*^{Q54} and MES mouse models of epilepsy.

GS967 prevents mossy fiber sprouting

Mossy fiber sprouting refers to the aberrant growth of granule cell axons (mossy fibers) into the inner molecular layer of the dentate gyrus.²¹ This phenomenon has been observed in patients with epileptic seizures and in animal models of epilepsy, but the contribution of mossy fiber sprouting to epileptogenesis remains unclear and controversial. Substantial evidence supports the idea that the sprouted fibers form synapses on granule cells and generate recurrent excitatory circuits capable of perpetuating seizure activity.²¹ Attempts to inhibit mossy fiber sprouting using commonly prescribed AEDs, including the voltage-gated sodium channel inhibitor lamotrigine, have been largely unsuccessful.^{30–33} Inhibition of the mammalian target of rapamycin (mTOR) signaling pathway has been demonstrated to suppress mossy fiber sprouting in animal models of temporal lobe epilepsy.³⁴ Our results

appear to represent the first example of a sodium channel blocking drug with antiepileptic properties capable of preventing mossy fiber sprouting in an epileptic animal model.

CONCLUSION

We demonstrated antiepileptic activity for two preferential persistent sodium current blockers. We further demonstrated that GS967 is a potent and selective inhibitor of persistent current that suppresses seizure activity in two mouse models, dampens hippocampal neuronal excitability in a concentration dependent manner, prolongs survival of genetically epileptic mice, and prevents both hilar neuron loss and development of mossy fiber sprouting in these mice. Our findings provide evidence suggesting that preferential inhibition of persistent sodium current is an effective strategy for development of new AEDs.

Supplementary Material

Refer to Web version on PubMed Central for supplementary material.

Acknowledgments

The authors thank Brian Stafford, Nevena Mollova and Rachael Lansdown for assistance in determining drug concentrations and Clint McCollom for mouse husbandry. The authors would also like to thank Robert Macdonald for his critical review of this manuscript. This work was funded in part by a research grant from Gilead Sciences, Inc. to A.L.G., and by grants from the National Institutes of Health (NS032387 to A.L.G.; NS053792 to J.A.K.; F31NS077700 to N.A.H.). L.L.A. is recipient of a predoctoral fellowship grant from the PhRMA Foundation, and C.H.T. was supported by a postdoctoral grant from the Epilepsy Foundation.

REFERENCES

1. Annegers JF, Hauser WA, Elveback LR, Kurland LT. The risk of epilepsy following febrile convulsions. *Neurology*. 1979; 29:297–303. [PubMed: 571973]
2. Leonardi M, Ustun TB. The global burden of epilepsy. *Epilepsia*. 2002; 43(suppl 6):21–25. [PubMed: 12190974]
3. Sander JW. The epidemiology of epilepsy revisited. *Curr Opin Neurol*. 2003; 16:165–170. [PubMed: 12644744]
4. Stafstrom CE. Persistent sodium current and its role in epilepsy. *Epilepsy Curr*. 2007; 7:15–22. [PubMed: 17304346]
5. George AL Jr. Inherited channelopathies associated with epilepsy. *Epilepsy Curr*. 2004; 4:65–70. [PubMed: 15562308]
6. Kahlig KM, Lepist I, Leung K, Rajamani S, George AL Jr. Ranolazine selectively blocks persistent current evoked by epilepsy-associated Nav1.1 mutations. *Br J Pharmacol*. 2010; 161:1414–1426. [PubMed: 20735403]
7. Kahlig KM, Hirakawa R, Liu L, George AL Jr, Belardinelli L, Rajamani S. Ranolazine reduces neuronal excitability by interacting with inactivated states of brain sodium channels. *Mol Pharmacol*. 2014; 85:162–174. [PubMed: 24202911]
8. Bergren SK, Chen S, Galecki A, Kearney JA. Genetic modifiers affecting severity of epilepsy caused by mutation of sodium channel Scn2a. *Mamm Genome*. 2005; 16:683–690. [PubMed: 16245025]
9. Kearney JA, Plummer NW, Smith MR, et al. A gain-of-function mutation in the sodium channel gene Scn2a results in seizures and behavioral abnormalities. *Neuroscience*. 2001; 102:307–317. [PubMed: 11166117]

10. Belardinelli L, Liu G, Smith-Maxwell C, et al. A novel, potent, and selective inhibitor of cardiac late sodium current suppresses experimental arrhythmias. *J Pharmacol Exp Ther.* 2013; 344:23–32. [PubMed: 23010360]
11. Sicouri S, Belardinelli L, Antzelevitch C. Antiarrhythmic effects of the highly-selective late sodium channel current blocker GS-458967. *Heart Rhythm.* 2013; 10:1036–1043. [PubMed: 23524321]
12. Mistry AM, Thompson CH, Miller AR, Vanoye CG, George AL Jr, Kearney JA. Strain- and age-dependent hippocampal neuron sodium currents correlate with epilepsy severity in Dravet syndrome mice. *Neurobiol Dis.* Epub 2014 Jan 14.
13. Lossin C, Wang DW, Rhodes TH, Vanoye CG, George AL Jr. Molecular basis of an inherited epilepsy. *Neuron.* 2002; 34:877–884. [PubMed: 12086636]
14. Rhodes TH, Lossin C, Vanoye CG, Wang DW, George AL Jr. Noninactivating voltage-gated sodium channels in severe myoclonic epilepsy of infancy. *Proc Natl Acad Sci U S A.* 2004; 101:11147–11152. [PubMed: 15263074]
15. Kahlig KM, Rhodes TH, Pusch M, et al. Divergent sodium channel defects in familial hemiplegic migraine. *Proc Natl Acad Sci U S A.* 2008; 105:9799–9804. [PubMed: 18621678]
16. Thompson CH, Kahlig KM, George AL Jr. SCN1A splice variants exhibit divergent sensitivity to commonly used antiepileptic drugs. *Epilepsia.* 2011; 52:1000–1009. [PubMed: 21453355]
17. White HS, Franklin MR, Kupferberg HJ, Schmutz M, Stables JP, Wolf HH. The anticonvulsant profile of rufinamide (CGP 33101) in rodent seizure models. *Epilepsia.* 2008; 49:1213–1220. [PubMed: 18325020]
18. Frankel WN, Taylor L, Beyer B, Tempel BL, White HS. Electroconvulsive thresholds of inbred mouse strains. *Genomics.* 2001; 74:306–312. [PubMed: 11414758]
19. Sloviter RS. A simplified Timm stain procedure compatible with formaldehyde fixation and routine paraffin embedding of rat brain. *Brain Res Bull.* 1982; 8:771–774. [PubMed: 6182964]
20. Dudek FE, Sutula TP. Epileptogenesis in the dentate gyrus: a critical perspective. *Prog Brain Res.* 2007; 163:755–773. [PubMed: 17765749]
21. Buckmaster, PS. Mossy Fiber Sprouting in the Dentate Gyrus. In: Noebels, J.; Avoli, M.; Rogawski, M.; Olsen, R.; Delgado-Escueta, A., editors. *Jasper's Basic Mechanisms of the Epilepsies* [Internet]. Bethesda, MD: National Center for Biotechnology Information; 2012. Available from: <http://www.ncbi.nlm.nih.gov/books/NBK98174/>
22. Mantegazza M, Curia G, Biagini G, Ragsdale DS, Avoli M. Voltage-gated sodium channels as therapeutic targets in epilepsy and other neurological disorders. *Lancet Neurol.* 2010; 9:413–424. [PubMed: 20298965]
23. Vanoye CG, Lossin C, Rhodes TH, George AL Jr. Single-channel properties of human Nav1.1 and mechanism of channel dysfunction in SCN1A-associated epilepsy. *J Gen Physiol.* 2006; 127:1–14. [PubMed: 16380441]
24. Veeramah KR, O'Brien JE, Meisler MH, et al. De novo pathogenic SCN8A mutation identified by whole-genome sequencing of a family quartet affected by infantile epileptic encephalopathy and SUDEP. *Am J Hum Genet.* 2012; 90:502–510. [PubMed: 22365152]
25. Holland KD, Kearney JA, Glauser TA, et al. Mutation of sodium channel SCN3A in a patient with cryptogenic pediatric partial epilepsy. *Neurosci Lett.* 2008; 433:65–70. [PubMed: 18242854]
26. Estacion M, Gasser A, Dib-Hajj SD, Waxman SG. A sodium channel mutation linked to epilepsy increases ramp and persistent current of Nav1.3 and induces hyperexcitability in hippocampal neurons. *Exp Neurol.* 2010; 224:362–368. [PubMed: 20420834]
27. Chen S, Su H, Yue C, et al. An increase in persistent sodium current contributes to intrinsic neuronal bursting after status epilepticus. *J Neurophysiol.* 2011; 105:117–129. [PubMed: 20980543]
28. Lin WH, Gunay C, Marley R, Prinz AA, Baines RA. Activity-dependent alternative splicing increases persistent sodium current and promotes seizure. *J Neurosci.* 2012; 32:7267–7277. [PubMed: 22623672]
29. Sun L, Gilligan J, Staber C, et al. A knock-in model of human epilepsy in *Drosophila* reveals a novel cellular mechanism associated with heat-induced seizure. *J Neurosci.* 2012; 32:14145–14155. [PubMed: 23055484]

30. Pitkanen A, Nissinen J, Jolkkonen E, Tuunanen J, Halonen T. Effects of vigabatrin treatment on status epilepticus-induced neuronal damage and mossy fiber sprouting in the rat hippocampus. *Epilepsy Res.* 1999; 33:67–85. [PubMed: 10022367]
31. Cha BH, Silveira DC, Liu X, Hu Y, Holmes GL. Effect of topiramate following recurrent and prolonged seizures during early development. *Epilepsy Res.* 2002; 51:217–232. [PubMed: 12399072]
32. Nissinen J, Large CH, Stratton SC, Pitkanen A. Effect of lamotrigine treatment on epileptogenesis: an experimental study in rat. *Epilepsy Res.* 2004; 58:119–132. [PubMed: 15120743]
33. Buckmaster PS. Prolonged infusion of tetrodotoxin does not block mossy fiber sprouting in pilocarpine-treated rats. *Epilepsia.* 2004; 45:452–458. [PubMed: 15101826]
34. Buckmaster PS, Ingram EA, Wen X. Inhibition of the mammalian target of rapamycin signaling pathway suppresses dentate granule cell axon sprouting in a rodent model of temporal lobe epilepsy. *J Neurosci.* 2009; 29:8259–8269. [PubMed: 19553465]

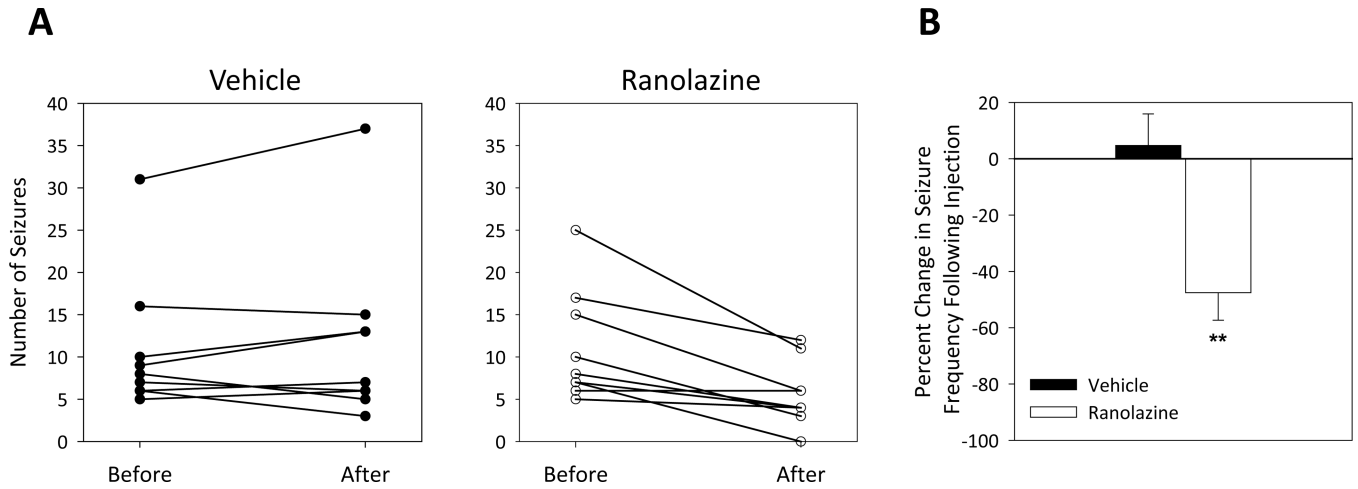


Figure 1. Ranolazine reduces seizure frequency in *Scn2a*^{Q54} mice

(A) Number of seizures for individual male mice in 30 minutes before and 30 minutes after treatment with either vehicle (*left*) or ranolazine (*right*). (B) A histogram of percent change in seizure frequency following a single i.p. injection of either vehicle or ranolazine (40 mg/kg). Percent change was calculated in response to treatment, with $n = 9$ for each treatment. (** $p < 0.005$; repeated measures ANOVA)

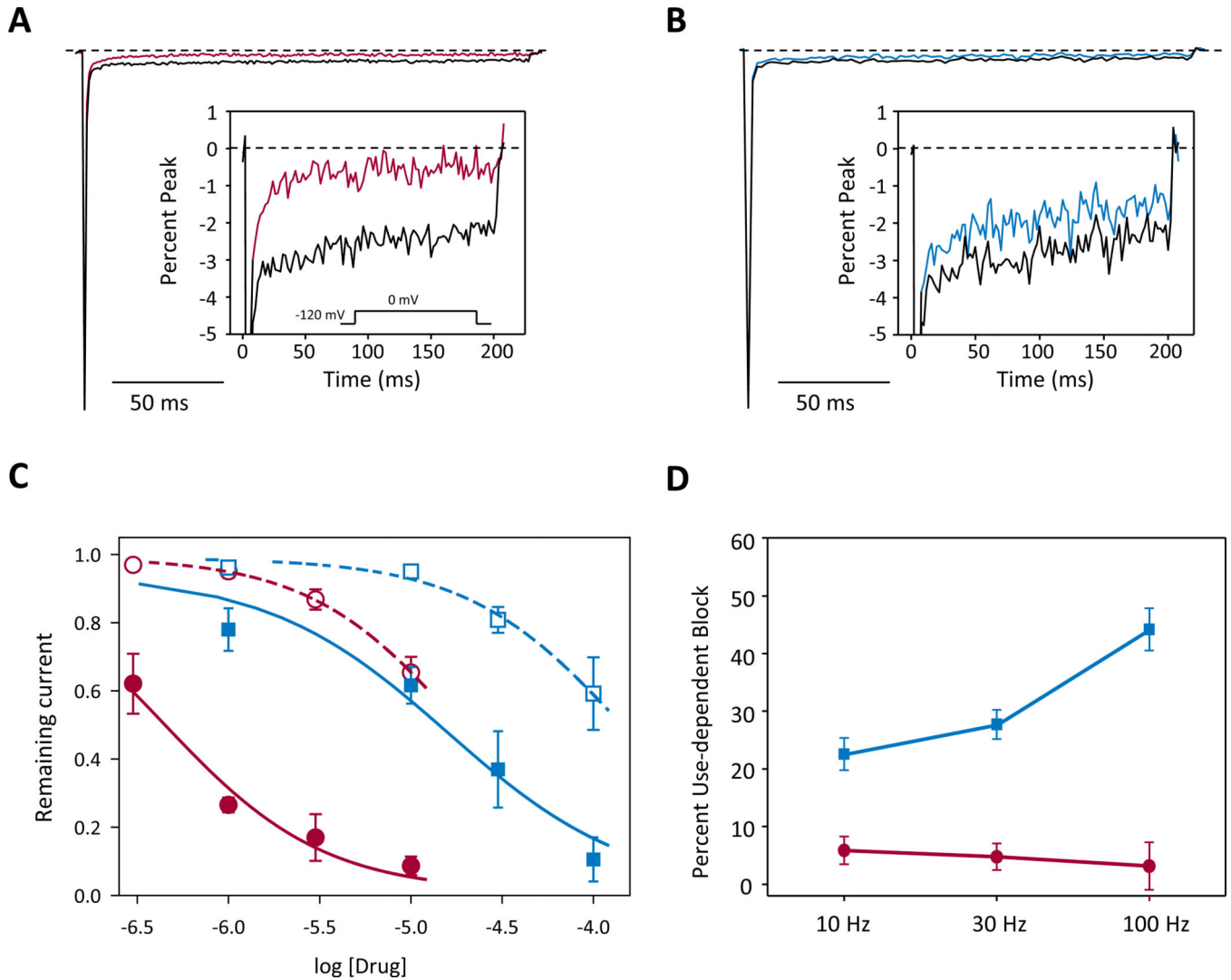


Figure 2. GS967 inhibits persistent sodium current

(A) Representative trace of sodium current in the absence (black trace) or presence (red trace) of 1 μM GS967. The inset illustrates persistent sodium current on an expanded scale. (B) Representative trace of voltage dependent sodium current in the absence (black trace) or presence (blue trace) of 10 μM phenytoin. The inset illustrates persistent sodium current on an expanded scale. (C) Concentration response of inhibition of persistent sodium current (closed symbols, solid lines) and transient sodium current (open symbols, dashed lines) by GS967 (red circles) and phenytoin (blue squares). (D) Steady-state use-dependent inhibition of transient sodium current by either 1 μM GS967 (red symbols) or 10 μM phenytoin (blue symbols) at stimulation frequencies of 10, 30, or 100 Hz. Values represent ratios of use-dependent inhibition in the presence of drug to that in the absence of drug. All data are expressed as mean \pm SEM, with $n = 7-11$ for each condition.

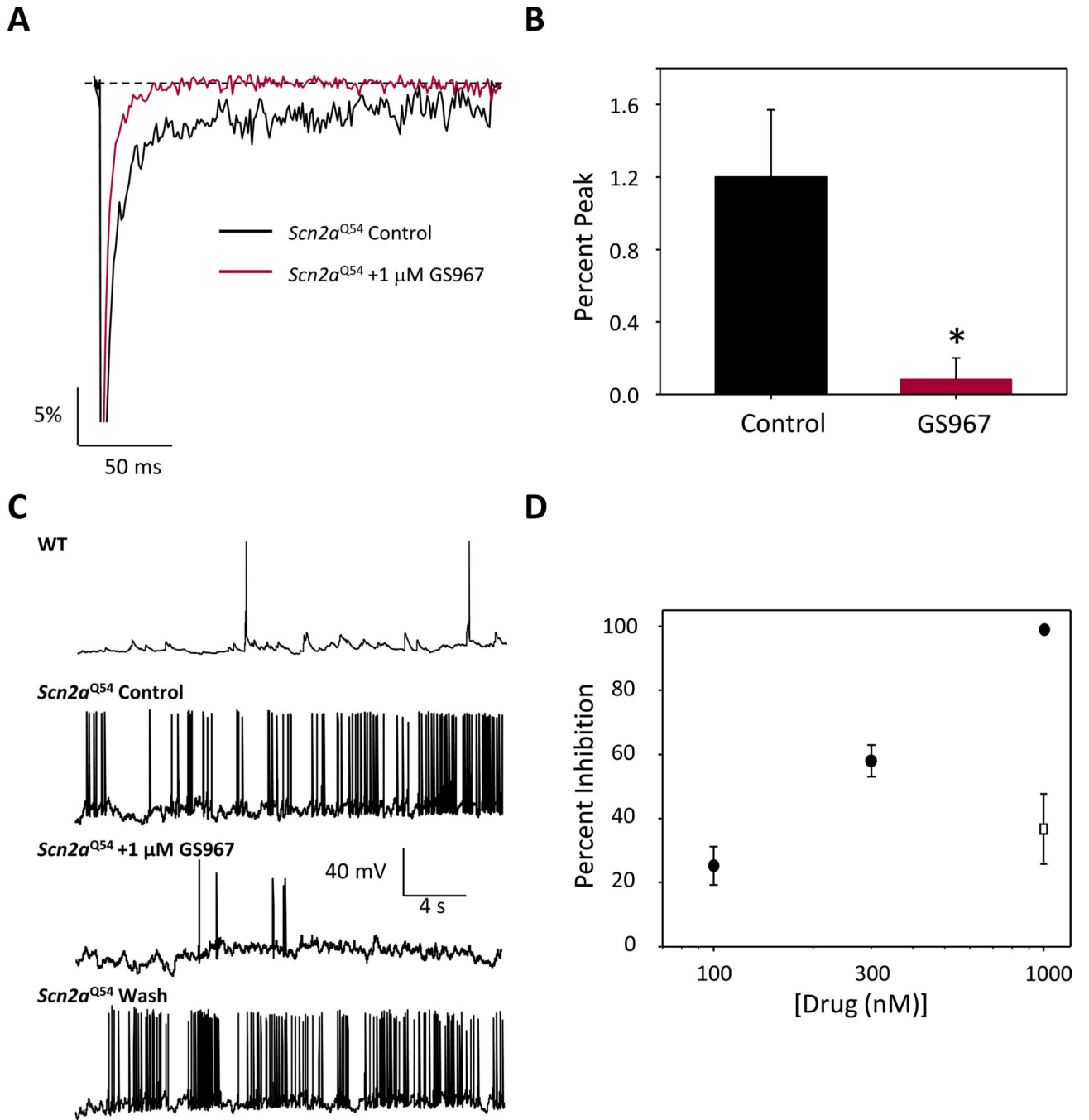


Figure 3. GS967 inhibits persistent current and spontaneous firing in *Scn2a*^{Q54} neurons
(A) Representative normalized trace of sodium currents from hippocampal pyramidal neurons from *Scn2a*^{Q54} mice recorded in the absence (black trace) or presence (red trace) of 1 μM GS967. **(B)** Summary data for persistent sodium current (expressed as % of peak current) recorded from pyramidal neurons in the absence or presence of 1 μM GS967. Peak current densities were not significantly different between control and GS967 conditions (control: 187.2 ± 32.6 pA/pF; GS967: 172.3 ± 46.2 pA/pF). **(C)** Representative spontaneous action potential firing recorded from a pyramidal neuron from either wild-type or *Scn2a*^{Q54}

mice. Membrane potential was clamped at -80 mV and spontaneous action potentials were recorded in the absence and presence of 1 μ M GS967. **(D)** Concentration response of inhibition of spontaneous action potential firing by GS967 (closed circles) and inhibition action potential firing by 1 μ M phenytoin (open square). Data are expressed as mean \pm SEM, with $n = 5-7$ for each concentration.

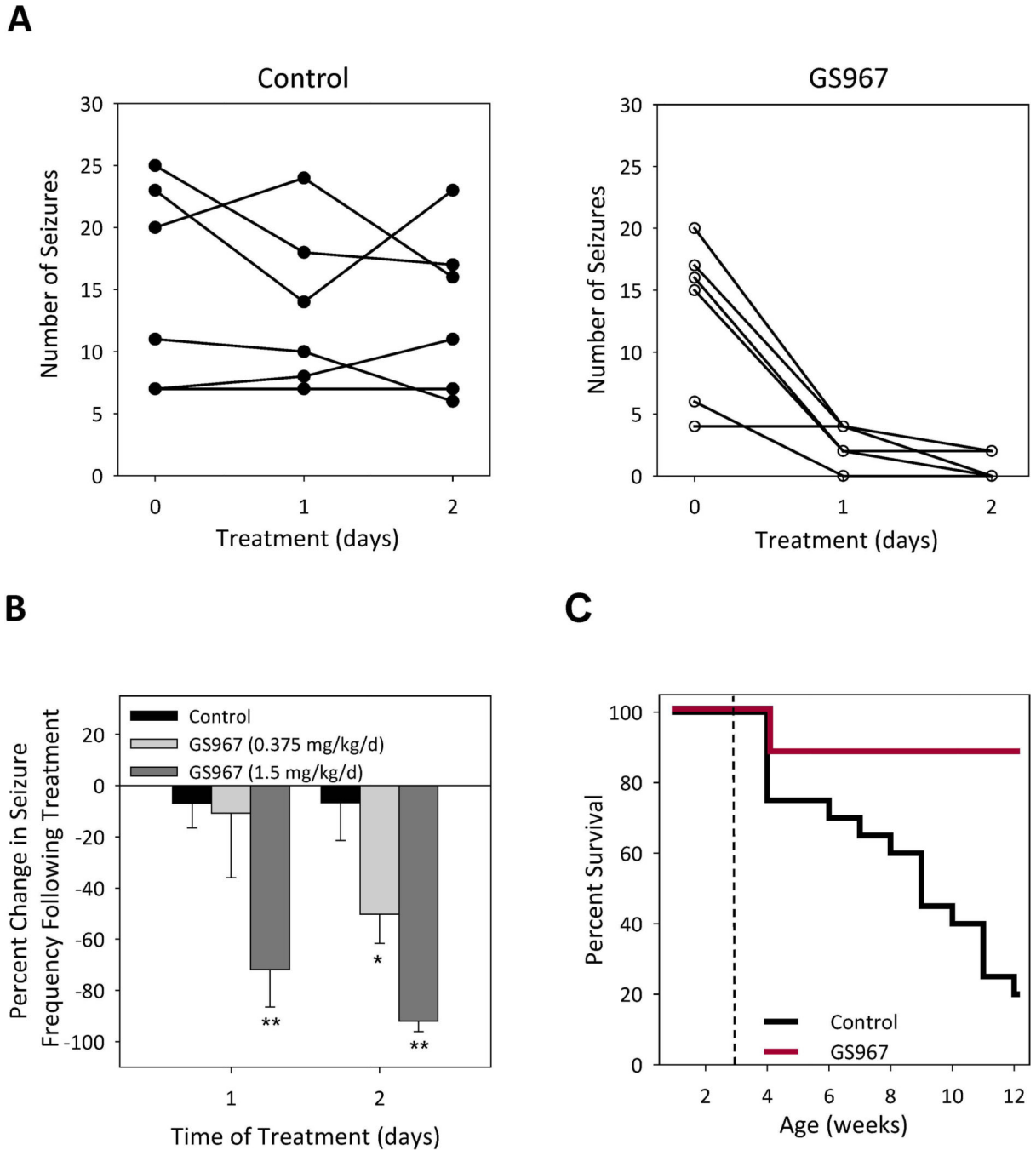


Figure 4. GS967 reduces seizure frequency and improves survival of *Scn2a*^{Q54} mice
 (A) Number of seizures in 30 minutes for individual mice at baseline (day 0) and after treatment (day 1 and 2) with either control chow or 1.5 mg/kg/d GS967. (B) A histogram of percent change in seizure frequency following oral administration of either control or chow containing GS967 at two dosage levels. Percent change was calculated in response to treatment, with $n = 6$ for each treatment ($*p < 0.05$ and $**p < 0.005$ compared to control; repeated measures ANOVA) (C) Survival curves of *Scn2a*^{Q54} mice placed on control chow or chow containing GS967 (dose 1.5 mg/kg/d). Treatment began at 3 weeks of age indicated

by the dashed line, with $n = 18\text{--}20$ per group. Survival difference between groups was significant at $p < 0.005$; Cox proportional hazards model.

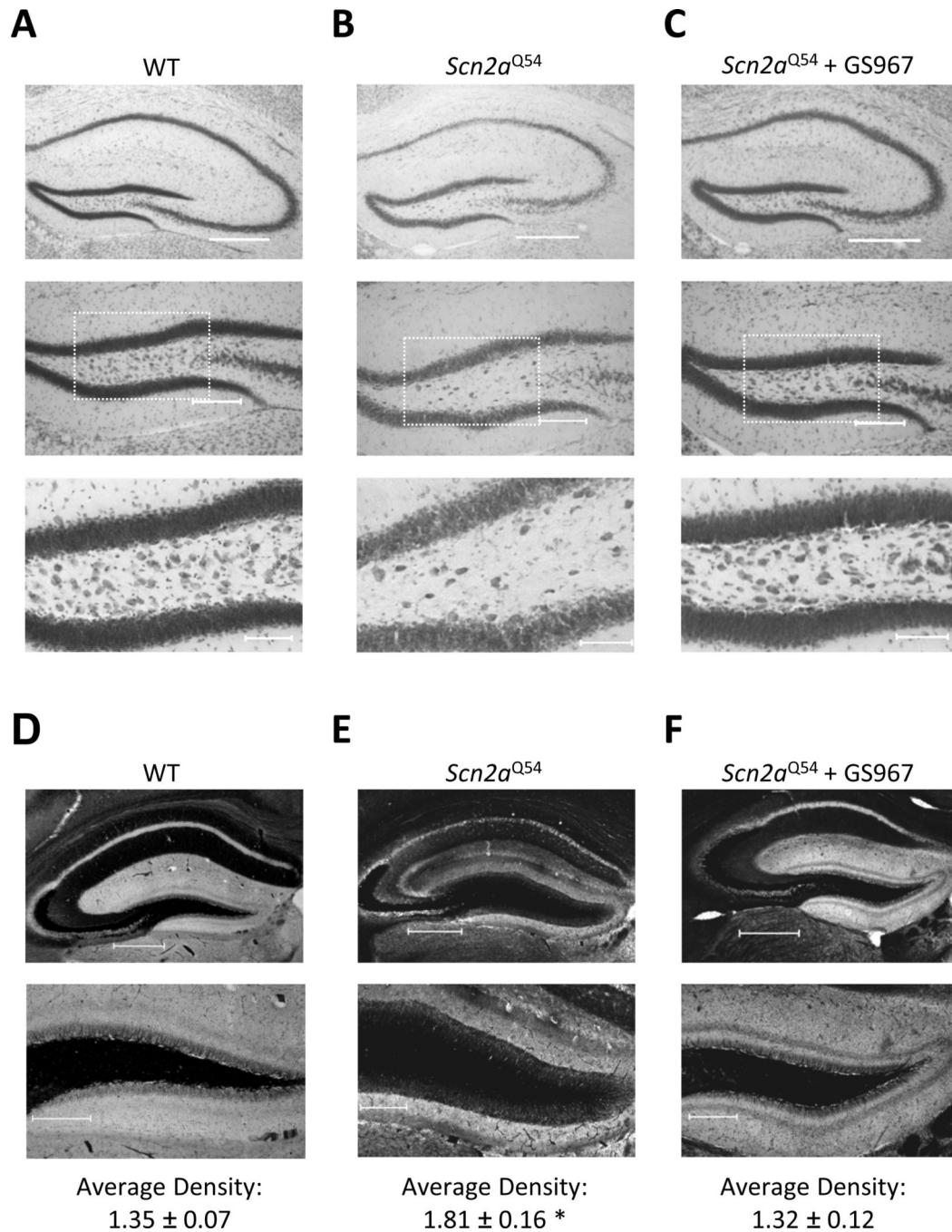


Figure 5. GS967 prevents hilar neuron loss and suppresses mossy fiber sprouting in *Scn2a*^{Q54} mice

A–C Cresyl violet stained sections of the dentate gyrus from a representative wild-type mouse (WT, panel **A**), untreated *Scn2a*^{Q54} mouse (panel **B**) and a *Scn2a*^{Q54} mouse treated with 1.5 mg/kg/d GS967 from P21-P60 (panel **C**). Images in the middle and lower panels are high-magnification views. Scale bars represent 500 μ m, 200 μ m and 100 μ m for the upper, middle and lower panels, respectively. **D–F**, Timm stained sections of the dentate gyrus from a wild-type (WT, panel **D**) untreated *Scn2a*^{Q54} mouse (panel **E**) and a *Scn2a*^{Q54}

mouse treated with GS967 from age P21-P60 (panel **F**). Images in the lower panels are high-magnification views. Scale bars represent 500 μm and 200 μm for the upper and lower panels, respectively. Quantification of the average density in the inner molecular layer of the dentate gyrus normalized to background is reported below images. Data are expressed as mean \pm SEM, with $n = 6-8$ per group ($*p < 0.05$; one-way ANOVA followed by Tukey's post-hoc).

Table 1

Plasma and brain concentrations

Drug [*]	Dosage (mg/kg) ^{**}	% Change in Seizure Frequency	[Plasma] [†]	[Brain]
Ranolazine	40	-48 ± 10%	19.3 ± 0.8 μM	4.9 ± 0.1 μM
Phenytoin	30	-93 ± 5%	87.2 ± 1.2 μM	ND
GS967	1.5	-92 ± 4%	0.6 ± 0.1 μM	0.6 ± 0.2 μM

* Ranolazine and phenytoin were administered as single i.p. injections. GS967 was orally administered through supplementation in chow.

** , GS967 dose is in units of mg/kg/day;

† phenytoin and GS967 are both highly (>90%) protein bound in plasma; ND, not determined